Charge dependence of electron emission in swift heavy-ion collisions with carbon

Michael Beuve, Michel Caron, Benoit Gervais, and Hermann Rothard
Centre Interdisciplinaire de Recherche Ions Lasers CIRIL (CEA-CNRS-ISMRA), BP 5133, Rue Claude Bloch, F-14070 Caen Cedex 05, France
(Received 17 April 2000)

We report on the charge dependence of electron yields from sputter-cleaned amorphous carbon targets bombarded with an isotachic set of swift ions. The experiments were performed in a UHV setup at the heavy-ion accelerator GANIL in Caen. The ion velocity was 19 a.u. (corresponding to a kinetic energy of 9.2 MeV/nucleon) and the projectile charge Q_P was varied from 6 to 39. As observed for ion-atom collisions, the electron yield exhibits a reduction with respect to a Q_P^2 law. We show that this projectile charge dependence is consistent with a strong saturation of low-energy primary electron ejection. This effect is related to the primary projectile-target interaction itself and not to high-charge effects affecting the electron transport before escape from the target.

I. INTRODUCTION

The major part of the kinetic energy lost by a swift ion in condensed matter is transferred to target electrons during the passage of the ion. Consequently, the subsequent kinetic electron emission from the solid surface is an important probe for the swift heavy-ion–solid interaction. Electron emission is usually regarded as a three-step process: *production* of electrons by primary ionization, *transport* of the electrons through the solid including secondary-electron production (cascade multiplication), and finally, *transmission* through the surface and ejection into the vacuum. Such a description can be modeled as a Markovian process for which the probability $f(\mathbf{r},\mathbf{v},t)$ to find an excited electron at a position $\mathbf{r}$ and a velocity $\mathbf{v}$ in the classical phase space is given by a master phase space equation.[1–3] For our purpose, we do not need to consider explicitly the details of this master equation. We simply write it as follows:

$$\frac{\partial f}{\partial t}+\mathbf{T}f=S(\mathbf{r},\mathbf{v},t). \tag{1}$$

S is the source term, which accounts for primary electron excitation via projectile-target interaction. $\mathbf{T}$ is an integro-differential operator, which accounts for the transport of the excited electrons through the foil. Since as a hypothesis the transport of an excited electron is regarded as diffusion in an unexcited material, the operator $\mathbf{T}$ is linear.[1–3] In the limit of the first Born perturbation theory, S is proportional to the squared projectile charge Q_P^2.[4] Since the left-hand side of Eq. (1) is linear, the number of excited electrons and hence the electron yield γ (the mean number of emitted electrons per incoming projectile) will be also proportional to Q_P^2. If such an assumption holds true, the ratio γ/Q_P^2 should be constant.

Obviously, electron transport and emission could be strongly influenced by the induced charge fluctuations in the ion's wake: due to a possible positive charging up of the track near the ion trajectory, slow electrons could be trapped in the ion's wake. This wake can be characterized by an induced track potential ϕ_{TR}.[5] Indeed, strong reductions of electron emission yields γ compared to such a Q_P^2 scaling have even been observed with fast, bare low-Z_P ions ($Z_P=1-8$) at high velocities (5 MeV/nucleon).[5] The reduction of low-energy electron emission has been also often explained by a screening of the projectile charge not only by the projectile electrons, but also by target electrons in metals.[6] However, such effects should be dominant at intermediate velocities of the projectile only, around and below the stopping power maximum, where also charge exchange effects come into play.

In order to explain these results with high-velocity bare ions, a model in terms of electron trapping in the wake of the ions was proposed by Borovsky and Suszcinsky[5] and refined by Benka *et al.*[7] The ion would create a positively charged zone in its wake, leading to an attractive track potential ϕ_{TR}, which results in an attractive force on the electrons moving away from the ion track. Consequently, electron yields would be reduced. The main prediction of the model is that the yield reduction becomes stronger with increasing Q_P for $v_P=\mathrm{const}$ because of the increasing ionization density. Since most of the secondary electrons originate from a small depth of the order of about 30 Å below the surface, another possible approach to explain electron yield reduction is to introduce a modified surface potential barrier $U=U_0+\Delta U$, where U_0 is the surface potential barrier in the limit of low ionization density and small electron yields.[8] For insulators, the underlying physical process is the creation of unbalanced positively charged holes in the wake of the ion. Because of the low electron mobility in insulators, the electronic relaxation may be many orders of magnitude (about 10^2-10^6 times) slower than in conductors.[9] Consequently, these holes cannot recombine within the escape time of the ion-induced emitted electrons and thus modify the planar surface potential by an additional ΔU. As was shown in Ref. 10, both approaches lead to formally similar expressions for the electron yield reductions: the induced change ΔU of the surface potential plays the role of the ion-induced track potential ϕ_{TR}. However, the predictions of such models clearly deviate strongly from experimental results in the case of highly charged swift heavy-ion impact on metals. The application of such kind of models seems to be more justified for

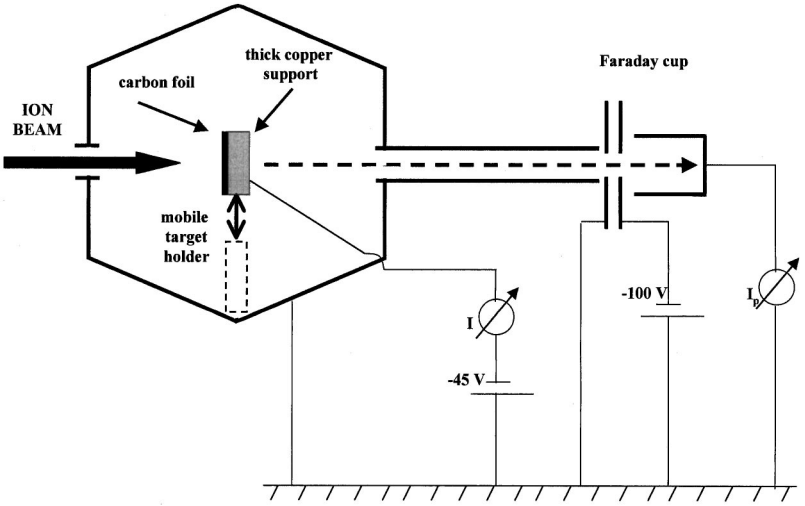

FIG. 1. Experimental setup (see text).

insulators.[9] It seems, however, that the considerations underlying these simple models suffer from a lack of rigorous knowledge of microscopic electron dynamics at a short time scale. In particular, it is worth keeping in mind that for any material the charged-particle wake field results from an accumulation of negative charges trailing the ion and screening it.[11]

Up to now, all of the high-energy experiments were performed with ill-defined surfaces in standard vacuum. Also, the experiments were restricted to bare low-Z_P ions ($Z_P = 1-8$) since it is important that the charge states Q_P of the incoming ions be close to their mean final charge $\langle Q_f \rangle$ in order to prevent preequilibrium effects connected to charge exchange. Indeed, while traveling through the solid, heavy ions may capture target electrons. Hence the projectile charge can be screened and the ion interaction cross section with the solid can be reduced. However, experiments with heavier ions should allow a more stringent test, since the models predict the strongest effects for MeV/nucleon heavy ions.

In order to obtain more reliable data on the backward yield dependence on projectile charge, we therefore measured electron yields in a ultrahigh-vacuum setup from sputter-cleaned surfaces of amorphous carbon with swift highly charged ions which fulfill the above conditions. In our analysis of the data, we ask whether it is necessary to introduce models dealing with a charged wake or electron trapping. Indeed, ''reduced'' electron yields may be simply related to deviations of the primary target ionization cross section (the source term S in the models) from a simple Q_P^2 scaling.

II. EXPERIMENT

The experiment was performed in an ultrahigh-vacuum setup especially designed for experiments at large-scale accelerators as described extensively elsewhere,[13] at the medium-energy beamline (SME) of the French heavy-ion accelerator GANIL in Caen. The velocity of ions was held constant at 19 a.u. (i.e., at a kinetic energy corresponding to 9.2 MeV/nucleon), while the charge of the projectile was varied from 6 to 39. The charge state of the incoming ions was chosen very close to the equilibrium charge in order to exclude effects connected to penetration depth dependent ion charges (see Table I).

Here we report the results of measurements of the backward electron yield γ_B from carbon targets. A schematic diagram of the experimental setup for electron yield measurements is shown in Fig. 1. The ejected electrons and the ion beam itself induce an electrical current in the target. The beam is stopped inside the target and generates a positive current I_P, and the induced electron emission creates a current I_e. Hence the measured target current I is

$$I = I_P + I_e . \tag{2}$$

The target is biased to a negative potential of approximately -45 V in order to ensure that all emitted electrons leave the target surface. Two Faraday cups upstream and downstream of the target allow measuring the ion beam intensity I_P when the target is removed from the beam path. The projectile flux (the number of projectile ions per second) ϕ_P can be calculated from the ion beam current I_P and the projectile charge Q_P (with e the unit of charge):

$$\phi_P = \frac{I_P}{eQ_P}. \tag{3}$$

In our experiment at GANIL, the beam is sufficiently stable in time to allow for such a procedure. Typically, one measurement cycle consists of a 200 s integration on the target and another 200 s integration with the Faraday cups. We repeat this cycle 10 times to get statistically meaningful current values.

The backward electron yield, defined as the mean number of electrons emitted from the beam entrance side of the target per incoming projectile,

$$\gamma_B = \frac{I_e}{e\phi_P}, \tag{4}$$

can then finally be calculated from

$$\gamma_B = \frac{I - I_P}{I_P} Q_P . \tag{5}$$

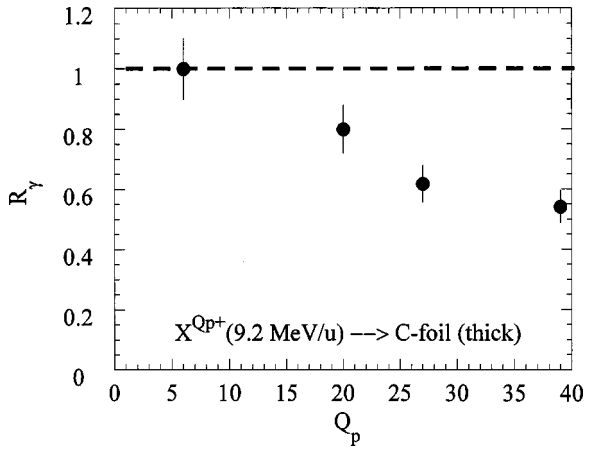

FIG. 2. Normalized yield R_γ of backward emitted electrons induced by ions impinging on a thick carbon foil with a kinetic energy corresponding to 9.2 MeV/nucleon. Comparison between the experimental data of Table I (solid circles) and Q_p^2 extrapolation (dashed line).

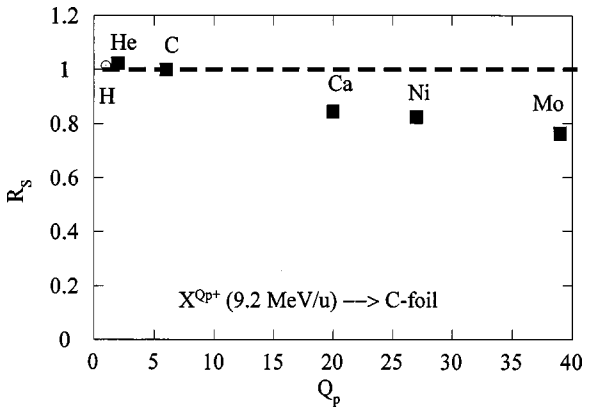

FIG. 3. Normalized stopping power R_S of ions impinging on carbon solid with a kinetic energy corresponding to 9.2 MeV/nucleon. Data of Table I: open circle (from Ref. 17), solid squares (from Ref. 16). Q_p^2 extrapolation: dashed line.

The main sources of error are the beam intensity fluctuations and we estimate the error to be less than $\pm 10\%$ of the measured value.[14]

The amorphous carbon used here can be considered as a good electrical conductor. Target foils of at least 300 μg/cm^2 (approximately 1.7 μm, density $\rho = 1.65$) were produced by standard evaporation techniques and mounted on copper supports thick enough to stop the ion beams at this energy. We note that the foils are thick enough to ensure that backward electron yields do not depend on the carbon foil thickness.[15] Before each measurement, we have controlled the surface contamination by Auger analysis. If contaminant peaks (oxygen) were seen, the target surface was sputter cleaned with 500 eV Ar^{1+} ions (5 μA for about 20 min). This process was repeated until no more contamination was observed. The total pressure inside the chamber during the measurement was about 5×10^{-10} mbar.

III. RESULTS AND DISCUSSION

In order to study the relative variations with the projectile charge Q_P, we define a normalized yield

$$R_\gamma = \frac{6^2 \gamma_B(Q_P)}{Q_P^2 \gamma_B(6)}, \tag{6}$$

so that $R\gamma = 1$ for $Q_P = 6$.

This ratio is presented in Fig. 2 as a function of Q_P. The dashed line indicates the expected linearity from Eq. (1) when the yield is linear in the source term and when the first Born approximation is applied in the source term calculations. In contrast, the measured R_γ values clearly decrease. The normalized yield for Mo^{39+} reduces to about half of the normalized yield for C^{6+}.

The discrepancy between experiment and theory could either come from the source term S or from a deviation from linearity of Eq. (1). In other words, it can either be connected to the ion-solid primary interactions or to nonlinear effects in the electron transport through the solid. As mentioned in the Introduction, in order to explain such a deviation, nonlinear transport mechanisms connected to a ''track potential''[5] or a ''microscopic surface potential''[6] were suggested. Nevertheless, a quantitative analysis shows that the related models yield unphysical values for the calculated potentials.[10] If, on the other hand, a primary ionization effect is involved, the validation of such a hypothesis requires observing the evolution of the stopping power with the projectile charge.

Therefore, we show in Fig. 3 a normalized stopping power defined in the same way as the normalized yield:

$$R_S = \frac{6^2 \mathrm{Se}(Q_P)}{Q_P^2 \mathrm{Se}(6)}. \tag{7}$$

The data are obtained by linear interpolation of the tables of Hubert *et al.*[16] for helium to molybdenum and of the ICRU tables[17] for hydrogen. These tables are the result of empirical formula fitted to a compilation of various experimental data performed with ions in charge state equilibrium. Compared to the empirical formula of Ziegler *et al.*,[18] these tables are in better agreement with experimental data in particular for heavy ions. Whereas the Q_P^2 extrapolated R_S is obviously a constant; the results from Refs. 16 and 17 decrease in the same way as the normalized electron yields of Fig. 2. Consequently, but without definitely excluding nonlinear transport effects, this comparison clearly points out that at least a part of the observed decrease of R_γ can be attributed to nonlinear primary effects in the projectile-target interaction itself. Among the possible primary effects, we have checked whether electron capture could play a role and we calculated the percentage of 9.2 MeV/nucleon ions that have reached a charge Q_P equal to the incident charge of the projectile after a distance of 1 μg/cm^2.[12] Indeed it has been shown theoretically[3] and experimentally[10] that the backward yield increases with the foil thickness until at a certain thickness a saturation is reached. In the case of amorphous carbon target the yield reaches about 90% of its maximal value for a thickness of the order of 1 μg/cm^2.[3] The calculated values are presented in Table I. From these values it seems that the capture mechanism plays a negligible role on the backward yield evolution with the incident charge of the projectile in our case. However, one could suggest that the projectile electrons could play a ''static role'' by simply modifying the

TABLE I. Backward yields and stopping powers for ions impinging on carbon solid with a velocity corresponding to 9.2 MeV/nucleon. The yields were measured with an incident charge Q_p close to the mean charge at equilibrium. The stopping powers are linear interpolations of the tables of Hubert *et al.* Ref. 16 (He–Mo) and Ref. 17 (H). Estimation (Ref. 12) of the mean charge $\langle Q_p \rangle$ at charge-state equilibrium and percentage estimation of ions still having a charge Q_p equal to the incident charge at the thickness 1 μg/cm^2 for a 2 g/cm^3 carbon solid density.

Ion	Q_p	γ_B	dE/dx (keV/μm)	$\langle Q_p \rangle$	$\%(Q_p=Q_{p0})$ at 1 μg/cm^2
H	1	-	8.730	1.00	100
He	2	-	35.00	2.00	100
C	6	3.6	307.6	5.99	99.95
Ca	20	32.0	2882	19.66	99.2
Ni	27	45.0	5128	26.5	98.8
Mo	39	82.3	9912	39.2	97.4

projectile potential felt by the target electrons. Nevertheless, such an effect cannot explain the reduction of the yield for the totally stripped Ca^{20+} projectile with no electrons present (see Table I).

Similar observations were made in ion-atom collisions, for stopping powers, ionization cross sections,[19] and excitation cross sections.[20] It was shown that such a so-called ''saturation effect'' (sometimes also called the ''nonlinear effect'') is not predicted by the first Born approximation, which would end up as a Q_P^2 law and is only valid for small perturbations. It is then conceivable that this ''saturation effect'' observed in ion-atom collisions also takes place in a solid target, where, however, the electronic structure of the target and consequently the interaction cross sections are different. In order to verify qualitatively this hypothesis and to quantify the correlation between the evolution of electron yield and stopping power with the projectile charge, we develop in the following a phenomenological model based on two assumptions only.

First, we assume a linear relation between the backward electron yield γ_B and the part of the projectile energy loss which goes into the ejection of low-energy primary electrons ($<$50 eV with respect to the vacuum level) within the typical escape depth of the low-energy electrons. This assumption is quite reasonable, since the backward yield mostly consists of low-energy electrons[21] from primary ionization.[3] We can write this relation as

$$\gamma_B = \frac{1}{A} \mathrm{Se}_l^{Q_p}, \tag{8}$$

where $\mathrm{Se}_l^{Q_P}$ represents the contribution of the stopping power of a Q_P-charged ion to the ejection of low-energy primary electrons and where A is a constant which depends on the target nature. This hypothesis corresponds to the treatment given by Schou,[22] but is somewhat different to the hypothesis of Sternglass,[23] which simply assumed proportionality between electron emission and the total stopping power of the projectile. Indeed, $\mathrm{Se}_l^{Q_P} dx$ should be used because the fast primary electrons escape the thin layer dx without losing a significant amount of energy and thus without producing a significant contribution to the backward yield.

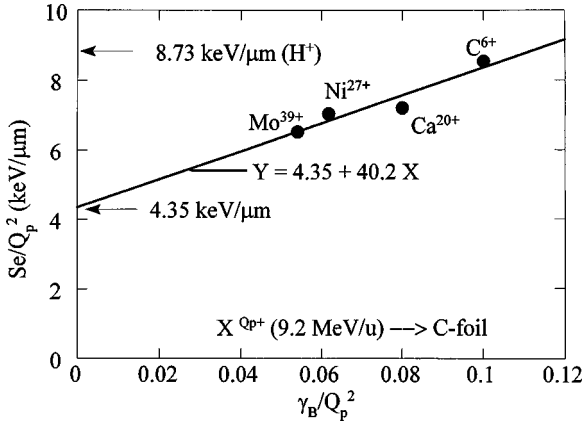

FIG. 4. Stopping power (normalized to the square of the ion incident charge) vs the backward emitted electron yield (also normalized to the square of the ion incident charge). The ions impinge on a thick carbon foil with an energy of 9.2 MeV/nucleon and with an incident charge Q_p close to the mean charge at charge-state equilibrium.

Second, we assume that the ejection of high-energy electrons is not affected by nonlinear effects and scales as Q_p^2. In ion-atom collisions, the saturation of electron energy differential cross sections with respect to the Q_p^2 scaling law concerns essentially collisions leading to low energy transfers.[3] This is consistent with the findings of such a scaling for ion-solid collisions.[24] This means that the contribution of the ejection of low-energy primary electrons to the total stopping power should be more significantly affected by the reduction effects than the contribution to the ejection of high-energy primary electrons. Thus the contribution of the stopping power of a Q_p-charged ion to the ejection of high-energy primary electrons $\mathrm{Se}_h^{Q_p}$ can simply be written as

$$\mathrm{Se}_h^{Q_p} = Q_p^2 \mathrm{Se}_h^{\mathrm{H}^+}. \tag{9}$$

From both assumptions, Eqs. (8) and (9), it follows that

$$Y = AX + B,$$

$$X = \frac{\gamma_B}{Q_p^2}, \quad Y = \frac{\mathrm{Se}^{Q_p}}{Q_p^2}, \quad B = \mathrm{Se}_h^{\mathrm{H}^+}. \tag{10}$$

Figure 4 shows the experimental set of (X,Y) couples on which the relation given by Eq. (10) was adjusted with the help of a least-mean-squares fit. Incontestably, Eq. (10) is well suited to describe the entire set of experimental data, thus strongly supporting the above made assumptions. Let us note that the present set of experimental data clearly excludes a linear relation between the stopping power and the backward yield. This is in agreement with the conclusions of Rothard *et al.*[10] based on other experimental data. These data were, however, obtained with ions of different velocities and ill-defined surface conditions. A linear relationship, often assumed in the literature, was established from simple macroscopic descriptions.[21–23] In our simple model, we rather propose the relation

$$\Lambda_B = \frac{\gamma_B}{\mathrm{Se}^{Q_P}} = \frac{X}{Y} = \frac{1}{A}\left[1 - B\frac{Q_p^2}{\mathrm{Se}^{Q_P}}\right]. \quad (11)$$

The backward electron yield is proportional to $\mathrm{Se}_l^{Q_p}$ and not to the total stopping power Se^{Q_p} because the charge dependences of $\mathrm{Se}_l^{Q_p}$ and $\mathrm{Se}_h^{Q_p}$ are different.

We can remark that the coefficient B, which is equal in our model to $\mathrm{Se}_h^{\mathrm{H}+}$, is of the order of $0.5\mathrm{Se}^{\mathrm{H}+}$ in agreement with the equipartition rule[21,23,25] valid at very high projectile velocity. The relation between B and $\mathrm{Se}^{\mathrm{H}+}$ should depend on the velocity only, while A depends only on the target properties. Let us note that an estimation using the first Born approximation within the dielectric formalism[11,26] yields $B = 0.7\mathrm{Se}^{\mathrm{H}+}$ (Refs. 3 and 27) with Ashley's dielectric function[28] for amorphous carbon at the same projectile velocity. On the other hand, for 2–8 MeV protons a simple semiempirical model adjusted on experimental data yields approximately $B = 0.4\mathrm{Se}^{\mathrm{H}+}$.[15] Several reasons may explain these differences. We particularly stress the quite arbitrary separation of ''low-energy'' and ''high-energy'' electrons in the second assumption, and the fitting procedure does not provide any information about this separation. Nevertheless, the good description of the experimental data by the simple model, Eq. (10), is a strong argument in favor of the interpretation that the first Born approximation is not valid for high charges.[19]

IV. CONCLUSION

We presented measurements of ion-induced backward electron emission yields as a function of the projectile charge. Swift ions at the same velocity impinged on amorphous sputter-cleaned and Auger-spectroscopy-controlled carbon targets. The ions were chosen with an incident charge Q_P as close as possible to the mean charge at equilibrium over a wide range of charge. We have shown that the experimental results deviate from the Q_P^2 law which results from standard microscopic models based on the first Born approximation and a linear transport equation. This reduction of the backward yield with respect to a Q_P^2 law is correlated with the evolution of the stopping power with Q_P without being strictly proportional to it. We developed a simple phenomenological model which shows explicitly the correlation between γ_B/Q_p^2 and Se/Q_p^2. Therefore the behavior of the backward emission yield with respect to Q_P can be interpreted as a primary effect independent of any transport effect. In particular, our model assumes a reduction of the low-energy primary electron ejection and in this sense it suggests that the observed effect is of the same nature as the so-called ''saturation effect'' observed in ion-atom collisions. Finally, our model proposes a simple charge-dependent relation between the stopping power and the backward electron yield, which fully accounts for the reduction effect in charge dependence.

[1] M. Rösler and W. Brauer, Phys. Status Solidi B **148**, 213 (1988); **104**, 161 (1981).

[2] A. Dubus, J. C. Dehaes, J. P. Ganachaud, A. Hafni, and M. Cailler, Phys. Rev. B **47**, 11 056 (1993).

[3] M. Beuve, Ph.D. thesis, University of Caen, 1999.

[4] M. R. C. McDowell and J. P. Coleman, *Introduction to the Theory of Ion-Atom Collisions* (North-Holland, Amsterdam, 1970).

[5] J. E. Borovsky and D. M. Suszcynsky, Phys. Rev. A **43**, 1433 (1991); **43**, 1416 (1991).

[6] A. Koyama, T. Shikata, H. Sakairi, and E. Yagi, Jpn. J. Appl. Phys., Part 1 **21**, 1216 (1982); **21**, 586 (1982).

[7] O. Benka, A. Schinner, T. Fink, and M. Pfaffenlehner, Phys. Rev. A **52**, 3959 (1995).

[8] M. Shi, D. E. Grosjean, J. Schou, and R. A. Baragiola, Nucl. Instrum. Methods Phys. Res. B **96**, 524 (1995).

[9] G. Schiwietz and G. Xiao, Nucl. Instrum. Methods Phys. Res. B **107**, 113 (1996).

[10] H. Rothard, M. Jung, J. P. Grandin, B. Gervais, M. Caron, A. Billebaud, A. Clouvas, R. Wünsch, C. Thierfelder, and K. O. Groeneveld, Nucl. Instrum. Methods Phys. Res. B **125**, 35 (1997); H. Rothard, M. Jung, M. Caron, J. P. Grandin, B. Gervais, A. Billebaud, A. Clouvas, and R. Wünsch, Phys. Rev. A **57**, 3660 (1998).

[11] P. M. Echenique, F. Flores, and R. H. Ritchie, Solid State Phys. **43**, 231 (1990).

[12] J. P. Rozet, C. Stephan, and D. Vernhet, Nucl. Instrum. Methods Phys. Res. B **107**, 67 (1996).

[13] M. Caron, H. Rothard, M. Jung, V. Mouton, D. Lelièvre, M. Beuve, and B. Gervais, Nucl. Instrum. Methods Phys. Res. B **146**, 126 (1998).

[14] There is one source of systematic error of such measurements which usually is neglected throughout the literature. Emitted electrons interact with the inner walls of the vacuum chamber. Low-energy electrons are absorbed by the grounded walls due to the target 45 V polarization, but high-energy electrons could be scattered back and induce an additional target current. However, fast electrons represent less than 10% of the whole emitted electrons, and the backscattering probability is about 25% [J. Schou, in *Physical Processes of the Interaction of Fusion Plasmas with Solids*, edited by W. Hofer and J. Roth (Academic, NY, 1996), p. 177]. Furthermore, we estimate from geometrical considerations that less than 5% of these electrons finally reach the target. Thus this effect can be neglected in comparison to the beam intensity.

[15] M. Jung, H. Rothard, B. Gervais, J. P. Grandin, A. Clouvas, and R. Wunsch, Phys. Rev. A **54**, 4153 (1996).

[16] F. Hubert, R. Bimbot, and H. Gauvin, At. Data Nucl. Data Tables **46**, 1 (1990).

[17] *Stopping Powers and Ranges for Protons and Alpha Particles*, ICRU Report 49 (ICRU, MD, 1993).

[18] J. F. Ziegler, J. P. Biersack, and U. Littmark, *The Stopping and Ranges of Ions in Solids, The Stopping and Ranges of Ions in Matter*, Vol. 1 (Pergamon, New York, 1985).

[19] P. D. Fainstein, V. H. Ponce, and R. D. Rivarola, J. Phys. B **21**, 287 (1988).

[20] D. Vernhet, L. Adoui, J. P. Rozet, K. Wohrer, A. Chetioui, A. Cassimi, J. P. Grandin, J. M. Ramillon, M. Cornille, and C. Stephan, Phys. Rev. Lett. **19**, 3625 (1997); D. Vernhet, J. P. Rozet, K. Wohrer, L. Adoui, C. Stephan, A. Cassimi, and J. M. Ramillon, Nucl. Instrum. Methods Phys. Res. B **107**, 71 (1996).

[21] D. Hasselkamp, H. Rothard, K. O. Groeneveld, J. Kemmler, P. Varga, and H. Winter, in *Particle Induced Electron Emission II*, edited by G. Höhler and E. A. Niekisch, Springer Tracts in Modern Physics Vol. 123 (Springer, New York, 1991).

[22] J. Schou, Scanning Microsc. **2**, 607 (1988); J. Schou, Phys. Rev. B **22**, 2141 (1980); P. Sigmund and S. Tougaard, *Electron Emission From Solids During Ion Bombardment: Theoretical Aspects*, Springer Tracts in Chemical Physics Vol. 17 (Springer, New York, 1981), p. 2.

[23] E. Sternglass, Phys. Rev. **108**, 1 (1957).

[24] M. Caron, H. Rothard, M. Beuve, and B. Gervais, Phys. Scr. **T80**, 331 (1999).

[25] N. Bohr, Mat. Fys. Medd. K. Dan. Vidensk. Selsk. **18**, No. 8 (1948).

[26] P. Nozières and D. Pines, Nuovo Cimento **9**, 470 (1958); P. Nozières, *Theory of Interacting Fermi Systems* (Benjamin, NY, 1964).

[27] B. Gervais and S. Bouffard, Nucl. Instrum. Methods Phys. Res. B **88**, 355 (1994).

[28] J. C. Ashley, J. J. Cowan, and R. H. Ritchie, Thin Solid Films **60**, 361 (1979).